EURASIP Journal on Wireless Communications and Networking
a SpringerOpen Journal

RESEARCH Open Access

An opportunistic cognitive radio communication through the exploitation of the small-scale fading mechanisms of the LTE mobile channel

Gerardo Agni Medina-Acosta[1*], José Antonio Delgado-Penín[1] and Katsuyuki Haneda[2]

Abstract

In recent years, the cognitive radio technology has attracted the attention of all the players in the telecommunication field (i.e., researchers, industry, service providers, and regulatory agencies) as a way of facing the spectrum scarcity. In this regard, and after having reviewed the vast activity linked to this concept it is quite easy to realize that the spectrum sensing task turns out to be the keystone of this technology. However, nowadays it is still unclear which is (are) going to be the globally recommended technique(s) for carrying out this procedure. So, and aiming at finding an alternative to the technical impediments behind the spectrum sensing task, this research work proposes that the advanced knowledge that is already being collected at the modern primary networks be used in benefit of the cognitive radios. Here, the 3GPP LTE network has been adopted as the primary system providing the information that the cognitive radio transceiver will be using for co-transmitting opportunistically (i.e., at specific moments) through the licensed radio resources, being the secondary access based on a novel model which proposes to overlay the secondary transmission whenever extreme channel conditions be found in the radio link of a particular primary user.

Keywords: Cognitive radio, Opportunistic communications, Passive awareness, Low impact interference, Induced interference, Multicarrier communication systems, 3GPP-LTE uplink, SC-FDMA

1. Introduction

The cognitive radio technology arose as a promising new paradigm in spectrum management aiming at overcoming the weakness embedded in the manner conventional radio devices communicate with each other at present.

In a broad sense, the idea behind this revolutionary technological proposal consists in making that the cognitive radio devices be able to transmit adaptively once a highly trustable sensing procedure in real time has guaranteed the existence of spectrum holes (at least in a four-dimensional basis, i.e., latitude, longitude, time, and frequency) which can freely be utilized under a double premise that consists in not causing excessive interference to the others, along with the mandatory release of the radio resources as soon as a user having higher hierarchy be back to the medium. In order to do so, a CoRa transceiver has to efficiently sensing its spectral environment, to understand it, to extract conclusions and learn about it, to discover its potential opportunities, to make decisions regarding its adaptability or reconfiguration, to guarantee its own QoS and the one of the others, while at the same time it keeps aware about any possible change within its RF medium.

Because all the implications stated above, this new generation of radio devices are considered to have cognition capabilities, being the so-called spectrum sensing task probably the most important, complex, and challenging procedure. In this regard, more than 10 years have already passed since the term cognitive radio was introduced to the telecommunications field, and nowadays a lot of scientific efforts are still ongoing trying to determine the most trustable techniques for performing the spectrum sensing task within the cognitive radio context. However, it could be inferred that many years (maybe more than a decade) are still for coming

* Correspondence: agni_medina@tsc.upc.edu
[1]Barcelona-Tech, Signal Theory and Communications Department, Technical University of Catalonia, Building D4, Campus Nord, Jordi Girona 31, 08034 Barcelona, Spain
Full list of author information is available at the end of the article

until we be able to embed practical solutions to all the challenges involved in the operation of a fully cognitive radio.

The motivation behind this research work lays in the fact of taking advantage of the information that nowadays is inherently being acquired at the modern primary networks. So, the cognitive radio communications would be implemented under an assisted detection scheme provided by the primary sites (i.e., base stations, backbone). This way, the primary infrastructure that has already been deployed would be reutilized in clever manner and in benefit of introducing the cognitive radio technology.

2. The cognitive radio and the LTE mobile channel

In this research work, an overlay communication mainly based on taking advantage of both time-varying nature of channel and frequency selectivity is utilized as a strategy for incorporating the cognitive radio technology into the 3GPP-LTE uplink system. Thus, and aiming at providing a clear understanding on how this model works, the following sections encompass the theoretical foundations behind this proposal, a brief review of the study object (i.e., LTE system), the description of the opportunistic cognitive radio model, and the testing scenario.

2.1. Principles of mobile radio communications

In a mobile communication system, the radio channels introduce randomness to the signal at the receiver as a result of the presence of two types of fading, which have been classified as large-scale fading and small-scale fading.

2.1.1. Large-scale fading

The large-scale fading deals with propagation models that estimate or predict the average signal power between a transmitter and a receiver over large distances (hundreds or thousands of meters), which turns out to be useful for estimating the coverage area of a transmitter. This kind of fading takes into account for the prominent natural and man-made formations (e.g., hills, forests, groups of buildings, etc.) which are typically found in the terrain that shelters a wireless communication link.

In literature, it is possible to find several models dealing with a variety of applications as well as environmental configurations for estimating the mean-path loss due to large-scale fading [1-4].

2.1.2. Small-scale fading

The small-scale fading is focused on propagations models whose aim is to characterize the drastic changes that can take place in the signal amplitude (in the order of 30 dB or 40 dB) over very short travel distances (e.g., half wavelength) or equivalent time durations (e.g., a few milliseconds) [5-9].

When the elements which propitiate the propagation mechanisms (e.g., reflection, diffraction, and scattering) are large in number (i.e., dense scatterer environment) and there is no line-of-sight, the power of the received signal as function of the antenna location behaves as dictated by a Rayleigh probability density function [10,11]. On the other hand, if there is a dominant component between the multiple arriving paths, then the received envelope and therefore the small-scale fading is described by a Rician probability density function [12,13].

2.1.2.1. Small-scale fading mechanisms The foundations of this proposal are directly related with the small-scale fading mechanisms known as delay-spreading of the signal and time-variance of the channel.

Delay spreading of the signal: This small-scale fading manifestation deals with the variations of the average received power as a function of the time delay.

When viewed in the time domain, it is said that a radio channel undergoes frequency-selective fading if the maximum excess delay T_m exceeds the symbol time T_s (i.e., $T_m > T_s$), which produces channel-induced intersymbol interference. Whereas if the opposite situation occurs (i.e., $T_m < T_s$), the channel would undergone flat or frequency-non-selective fading [14].

In turn, an analogous classification of the signal dispersion can be viewed in the frequency domain, categorizing the channel as frequency-selective fading if the coherence bandwidth f_0 is smaller than the signal bandwidth W (i.e., $f_0 < W \approx 1/T_s$), meaning that f_0 represents to be a very small frequency range compared with the occupied by W. Conversely, if $f_0 > W \approx 1/T_s$, then it can be assumed that all the signal's spectral components will be affected in a similar way by the channel (undergoing either fading or not fading) [15].

Time variance of the channel: This manifestation is produced due to the fact that the received multipath components are highly dependent on the signal frequency and on the position of the antenna. However, besides the variations due to the relative motion between the transmitter and receiver, the same time-variant behavior of the channel can be caused by the movement of surrounding objects.

In the time domain, the fading rapidity experienced by a channel is denominated as slow fading if the coherence time T_o is longer than the symbol time T_s (i.e., $T_o > T_s$), being inferred that the channel will remain the same during several or at least one transmitted symbol. In the opposite case (i.e., $T_o < T_s$), the fast fading takes place leading to several drastic changes in the channel while a symbol is being transmitted, which results in waveform distortions yielding irreducible error rates [16].

In the frequency domain, the slow fading happens when the signal bandwidth is greater than the spectral

broadening or Doppler spread (i.e., $W > f_d$ or approximately $1/T_s > 1/T_o$). When $W < f_d$, then the time-varying nature of the channel is described to as fast fading [17].

2.2. The LTE uplink and the mobile channel

Once a brief review of the small-fading mechanisms was given, a general view about the LTE mobile channel and the SC-FDMA system is provided in this section, this since both became in the study object of this proposal.

2.2.1. The LTE mobile channel

In the 3GPP technical specifications 45.005 V9.3.0 (2010–05), several propagation models (e.g., rural area, hilly terrain, etc.) are defined in terms of a set of taps, being each of them determined by a particular time delay and average power [18]. Concretely, the one defining the typical case for an urban area has been selected as study object of this proposal, which is shown in Table 1.

In terms of the small-scale fading mechanisms, the specifications shown in such a table (i.e., Power Delay Profile) refer to the time spreading of the signal. So, according to Section 2.1.2.1, and by assuming a correlation function above 0.5, the coherence bandwidth of the channel is approximately 199.5527 kHz, then the channel can theoretically be classified as frequency-selective given that the minimum LTE channel bandwidth is equal to 1.4 MHz, which clearly exceeds f_0. This is the reason why a variable length cyclic prefix (i.e., normal or extended) matching the time-slot (0.5 ms) is included in LTE [19].

Moreover, aiming at adding a time-varying nature to the channel described in Table 1, the generation of correlated Rayleigh fading depending on the Doppler frequency was implemented as described in [20], its block diagram is shown in Figure 1.

Table 1 Typical case for urban area: (12 tap setting)

Tap number	Relative time (μs)	Average relative power (dB)
1	0.0	−4.0
2	0.2	−3.0
3	0.4	0.0
4	0.6	−2.0
5	0.8	−3.0
6	1.2	−5.0
7	1.4	−7.0
8	1.8	−5.0
9	2.4	−6.0
10	3.0	−9.0
11	3.2	−11.0
12	5.0	−10.0

The model shown above represents to be an improvement (i.e., in terms of memory resources and number of executed operations) made to the algorithm originally presented by Smith [21] for generating correlated Rayleigh random variates. The process starts by giving as input two sequences (e.g., N equal to 10,000) composed of independent and identically distributed (i.i.d) Gaussian random variables having a zero mean and a variance according to the average relative powers given in Table 1, which represent, respectively, the real and imaginary parts of a single tap (i.e., the same procedure has to be repeated for each of the taps). Then by using the appropriated filter coefficients $F[k]$ (i.e., in accordance with the desired maximum Doppler frequency f_d, carrier frequency f_c, and UE speed V) the sequences $A[k]$ and $B[k]$ are weighted, being later on added in quadrature $X[k]$, to finally be transformed to the time domain $x[n]$ in order to provide the required complex baseband Rayleigh fading with Doppler shift.

Previously at the end of the last section it was mentioned that the coherence time determines the expected amount of time during which the channel's response can be considered as invariant. In this regard, there exists a typical rule of thumb for computing the coherence time as a function of the Doppler spread ($f_d = V/\lambda$), which is given as follows:

$$T_0 = \sqrt{\frac{9}{16\pi {f_d}^2}} \tag{1}$$

The above expression results from taking the geometric mean of the basic definition of the coherence time ($T_o \approx 1/f_d$), and its definition when it is assumed that the channel correlation is greater than 0.5 [22]. If we make use of the above so-called rule of thumb, and we consider a user equipment (UE) operating at 1850.7 MHz (E-UTRA uplink operating band 2), which is moving at a speed equal to 15 km/h, then we would obtain a T_o = 16.462 ms. That means that if we refer to the LTE standard [23], we could assume that under those conditions and if we consider for example a normal cyclic prefix in order to have seven symbols per time slot, then around 230 SC-FDMA symbols would be experiencing the same conditions (nulls, peaks, or something in between) until the channel changes again. In order to perceive this, the channel frequency response of the implemented mobile channel for the case of 128 subcarriers is shown in Figure 2.

From the above figure, it is possible to observe the presence of the frequency selectivity on the subcarriers, while the time-varying nature of the channel can be perceived through the different SC-FDMA transmitted symbols. Getting back to the coherence time issue, it can be seen that for 1380 SC-FDMA transmitted symbols (i.e., approximately 98.6 ms), the channel only changed six times

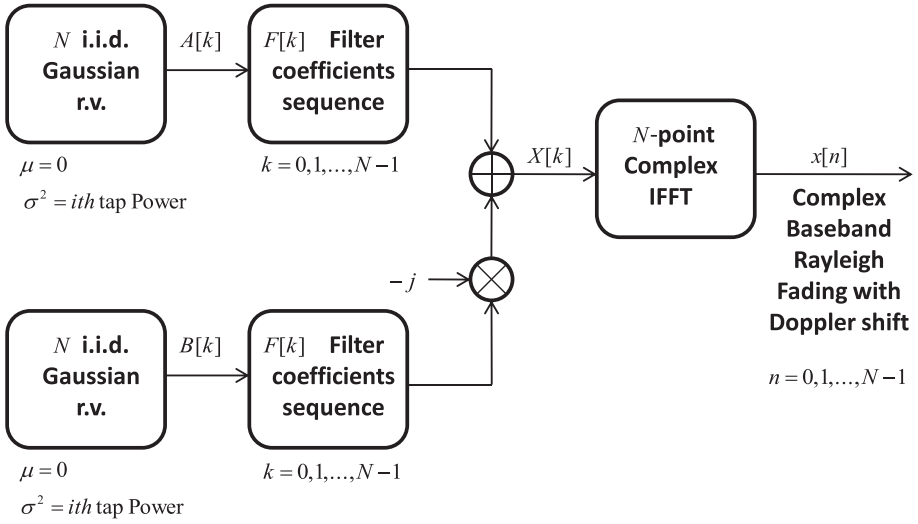

Figure 1 Block diagram of the algorithm proposed by Young and Beaulieu [20] for generating sequences of correlated Rayleigh variables.

(*y*-axis), remaining invariant approximately during 16.462 ms, and thus affecting groups of 230 SC-FDMA symbols in a constant manner.

2.2.2. The LTE uplink system

Once the LTE channel has been presented in terms of small-scale fading mechanisms, now the baseband block diagram of the SC-FDMA transceiver chain is shown in Figure 3.

At the transmitter, the procedure initiates in the time domain with the serial arranged symbols which are modulated, later on this information is set into parallel and fed to the *N*-point fast Fourier transform (FFT) which produces a set of modified complex numbers in the frequency domain. At this point the information has been spread out over the *N* subcarriers, subsequently a mapping procedure takes place in order to map one-on-one the modified complex numbers to a set of *N* contiguous subcarriers (zeros are placed into the *M*–*N* unused subcarriers), just after the *M*-point inverse fast Fourier transform is applied for transforming the information to the time domain, which is converted back to serial form for adding a cyclic prefix, letting this way the baseband SC-FDMA symbol ready to be transmitted through the channel [24,25].

Once the circular convolution between the SC-FDMA symbol and the channel took place, the set of initial steps at the receiver consist in removing the cyclic prefix, converting the information to parallel form, and utilizing the *M*-point FFT to transforming back the received information to the frequency domain, later on a de-mapping procedure is carried out aiming at strictly preserving the *N* subcarriers that were allocated to the user in question, which are equalized in order to provide a better estimation of the originally modified complex numbers, then they are transformed back to the time domain for obtaining the input needed by the de-modulator, which provides the recovered symbols that finally are rearranged in serial form [26,27].

2.3. Opportunistic secondary communication by exploiting the small-scale fading mechanisms of the LTE mobile channel

Until this point it is pretty clear that this proposal considers both the time-varying nature of channel and the frequency selectivity, for introducing a secondary communication into SC-FDMA system. Now, the following sections are focused on explaining in detail how this model works.

2.3.1. The overlay secondary communication model

As starting point, the frequency domain representation of a conventional transmission is given as follows:

$$Y(k) = H(k)X(k) + Z(k), \tag{2}$$

where $Y(k)$ represents the received signal on the kth subcarrier, $H(k)$ the channel gain, $X(k)$ the transmitted signal, and $Z(k)$ the AWGN sample. On the other hand, $\mathbf{Y}$ is by itself the whole SC-FDMA received symbol encompassing a set of subcarriers $\mathbf{X}$ that were distorted by the channel $\mathbf{H}$, as well as by the AWGN noise $\mathbf{Z}$.

In Section 2.2.2, it was mentioned that there is one equalizer included at the reception chain aiming at compensating the distortions produced by the channel. In this analysis, the well-known MMSE equalizer was considered to be embedded at the receptor, which provides a weighting factor on the kth subcarrier given by the following equation.

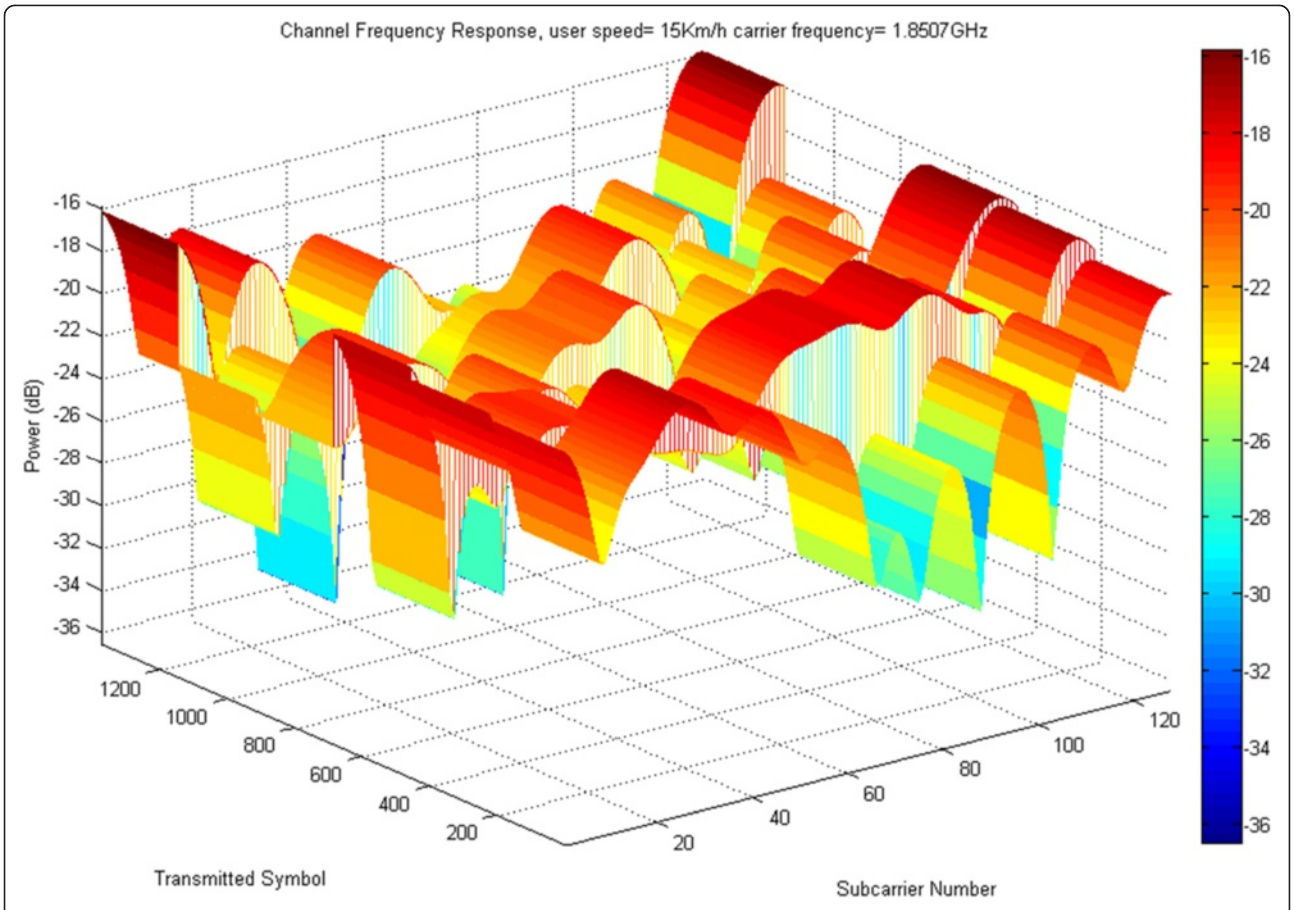

Figure 2 Channel frequency response model for a UE operating at 1850.7 MHz which is traveling at 15 km/h.

$$G(k) = \frac{H(k)^*}{|H(k)|^2 + \sigma^2}, \tag{3}$$

where * refers to the conjugate of the kth channel gain, and σ^2 to the AWGN noise variance. An important thing to highlight here is that the MMSE equalizer requires channel knowledge for its proper operation, information that according to the 3GPP-LTE is provided by eNode-B per every transmission time interval [28]. A view on one of the recovered subcarriers once the MMSE has acted on the received signal is shown next [29].

$$\hat{X}(k) = \frac{|H(k)|^2}{|H(k)|^2 + \sigma^2} X(k) + \frac{H(k)^*}{|H(k)|^2 + \sigma^2} Z(k) \tag{4}$$

The left-hand side of the above equation represents the signal, while the right-hand side refers to the noise, and therefore the signal-to-noise ratio at the receiver can be described as follows:

$$\mathrm{SNR}_{\mathrm{MMSE}}(k) = \frac{P\left(\frac{|H(k)|^2}{|H(k)|^2+\sigma^2}\right)^2}{\sigma^2\left(\frac{|H(k)|}{|H(k)|^2+\sigma^2}\right)^2} = \frac{P|H(k)|^2}{\sigma^2}, \tag{5}$$

where P refers to the power of the transmitted signal. A point to highlight here is that the signal-to-noise ratio is directly related with the channel conditions reported on the kth subcarrier.

Once the conventional transmission has been described, now the proposed model of a cognitive radio communication overlaid on the primary transmission will be described in detail.

According to this proposal, the deep fadings as well as the channel peaks will play the role of the extreme channel conditions to be tracked by cognitive radio user, which will be allow to co-transmitting strictly there (i.e., on the primary resources affected by such as extreme conditions).

According to this proposal, the deep fadings, as well as the channel peaks (i.e., extreme conditions) will be playing the role of the enablers for establishing

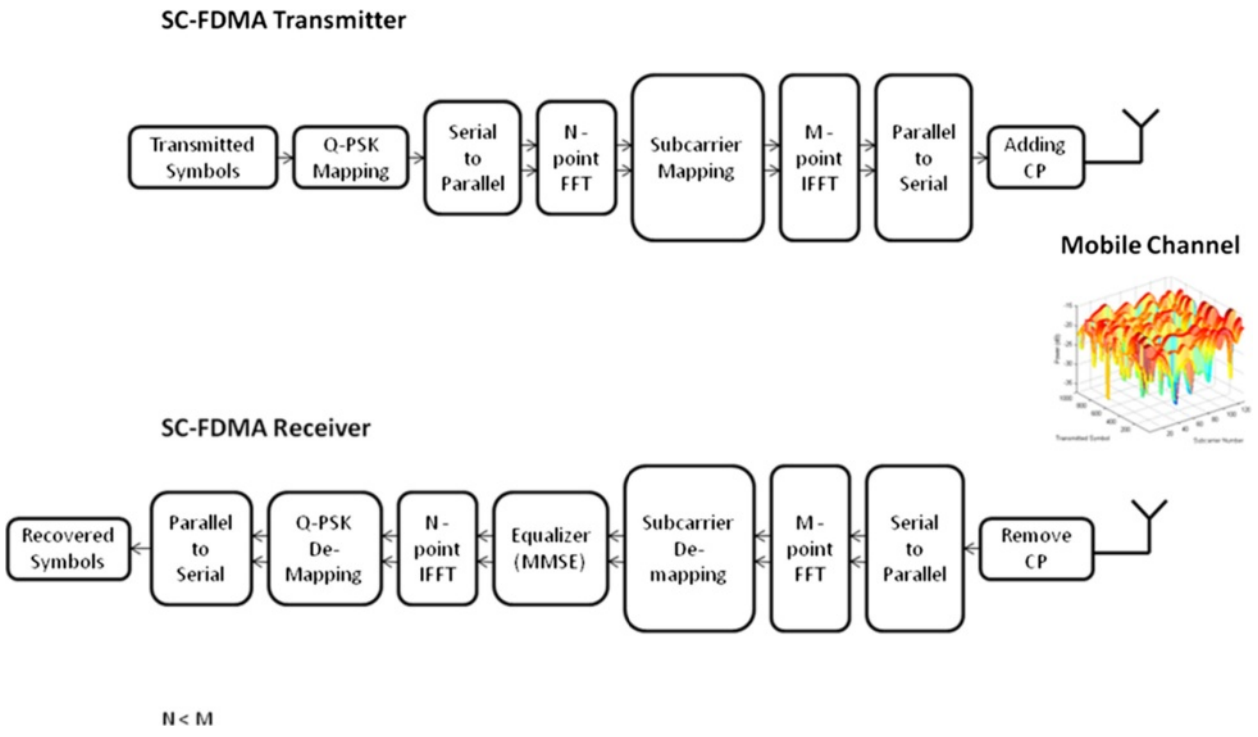

Figure 3 Transmitter and receiver structure of the SC-FDMA system.

opportunistic secondary communications by the cognitive radio user. That is, whenever a UE on the LTE system be undergoing very bad/good on a certain number of subcarriers, such a radio resources will be offered to the cognitive radio device for establishing an opportunistic communication in parallel.

Next it is shown how Equation (5) is modified when a cognitive radio communication is overlaid on the conventional transmission.

$$Y(k) = H(k)X(k) + Z(k) + H_{\mathrm{SU}}(\breve{k})X_{\mathrm{SU}}(\breve{k}), \quad \breve{k} \in k, \tag{6}$$

where H_{SU} and X_{SU} represent the channel and the transmitted information corresponding to the SU, respectively. Moreover, $\breve{k}$ emphasizes that only the subcarriers that are undergoing either a null or a peak (i.e., depending on the analysis) will be reutilized by the SU. The later means that the part of the equation above producing interference to the conventional transmission will only affect a limited number of subcarriers (<< to the total number of available subcarriers), and that can even disappear when no extreme conditions be found in the radio link being tracked by the SU.

So, under the overlay approach the estimated transmitted symbol after using the MMSE equalizer can be written as follows:

$$\hat{X}(k) = \frac{|H(k)|^2}{|H(k)|^2 + \sigma^2}X(k) + \frac{H(k)^*}{|H(k)|^2 + \sigma^2}Z(k) + \frac{H(k)^* H_{\mathrm{SU}}(\breve{k})}{|H(k)|^2 + \sigma^2}X_{\mathrm{SU}}(\breve{k}), \tag{7}$$

where the members of the above equation correspond to the signal, the noise, and the interference, respectively. Highlighting that from Equation (7) it is possible to describe the signal-to-interference ratio (SIR) on the kth subcarrier as follows:

$$\mathrm{SIR}_{\mathrm{MMSE}}(k) = \frac{P|H(k)|^2}{P_{\mathrm{SU}}\left|H_{\mathrm{SU}}(\breve{k})\right|^2}, \tag{8}$$

where P_{SU} refers to the transmitted power by secondary user. On the other hand, the signal-to-noise plus interference ratio can be rewritten as follows:

$$\mathrm{SNIR}_{\mathrm{MMSE}}(k) = P\left(\frac{|H(k)|^2}{\sigma^2 + P_{\mathrm{SU}}\left|H_{\mathrm{SU}}(\breve{k})\right|^2}\right) \tag{9}$$

Among other things, the equations shown above will allow us evaluating the impact that the overlaid cognitive radio communication will originate on conventional transmission.

2.3.2. Secondary overlay communication in a 3GPP-LTE multiuser environment

According to this proposal, instead of conducting a sensing procedure, the SU will be re-using the feedback information (i.e., the channel state information) provided by the primary base station. The above means that the SU will be aware of the PU nearest to its location aiming at accessing his resources in an opportunistic way and as a function of the reports delivered by the eNodeB. So, after an initial listening procedure and once a threshold has been established regarding the identification of the extreme conditions, the SU will conclude which subcarriers (over all the radio resources allocated to a particular PU) are undergoing the worst/best conditions (i.e., nulls or peaks depending on the analysis) in order to initiate a low-priority communication. So, and by reviewing the model description initiated in Section 2.3, it is important to highlight that at least four elements concerning to a cognitive process have been utilized: perception (primary network view), awareness (feedback awaiting), learning (coherence time estimation), and judgment (opportunistic transmission nulls/peaks). A schematic representation of this proposal is shown in Figure 4.

Figure 4a shows 128 available subcarriers in the system, which are split in four resource chunks in order to allocate four users simultaneously without co-channel interference. The SU will be tracking a particular user, and will access the resources opportunistically using the extreme channel conditions as an enabler.

Figure 4b illustrates how the SU only puts data over the subcarriers that are being a victim of an extreme channel condition (zeros are set elsewhere in order to avoid interfering). Figure 4c is focused in showing an opportunistic secondary transmission tracking the channel peaks, where we can see how after receiving the update by the eNodeB (tentatively every 1 ms) the SU will adapt his transmission without distorting the others.

In order to recreate a multiuser scenario, four mobile radio channels were implemented (i.e., one-by-one) as described in Section 2.2.1, being the main parameters (also extracted from the norm) summarized in Table 2 [23,30,31]. The implemented mobile channels are shown in Figure 5.

The above figure only gives a view from symbols 1150 to 2530 over a total of 10,000 SC-FDMA transmitted symbols (what is equivalent approximately to 98.6 ms), where it can be noticed the fluctuations produced as a function of the UE's speed (or UE's antenna position). In fact, it can be perceived that in the case of the UE moving at 15 km/h the channel only changed six times, opposite situation to the UE moving at 120 km/h for

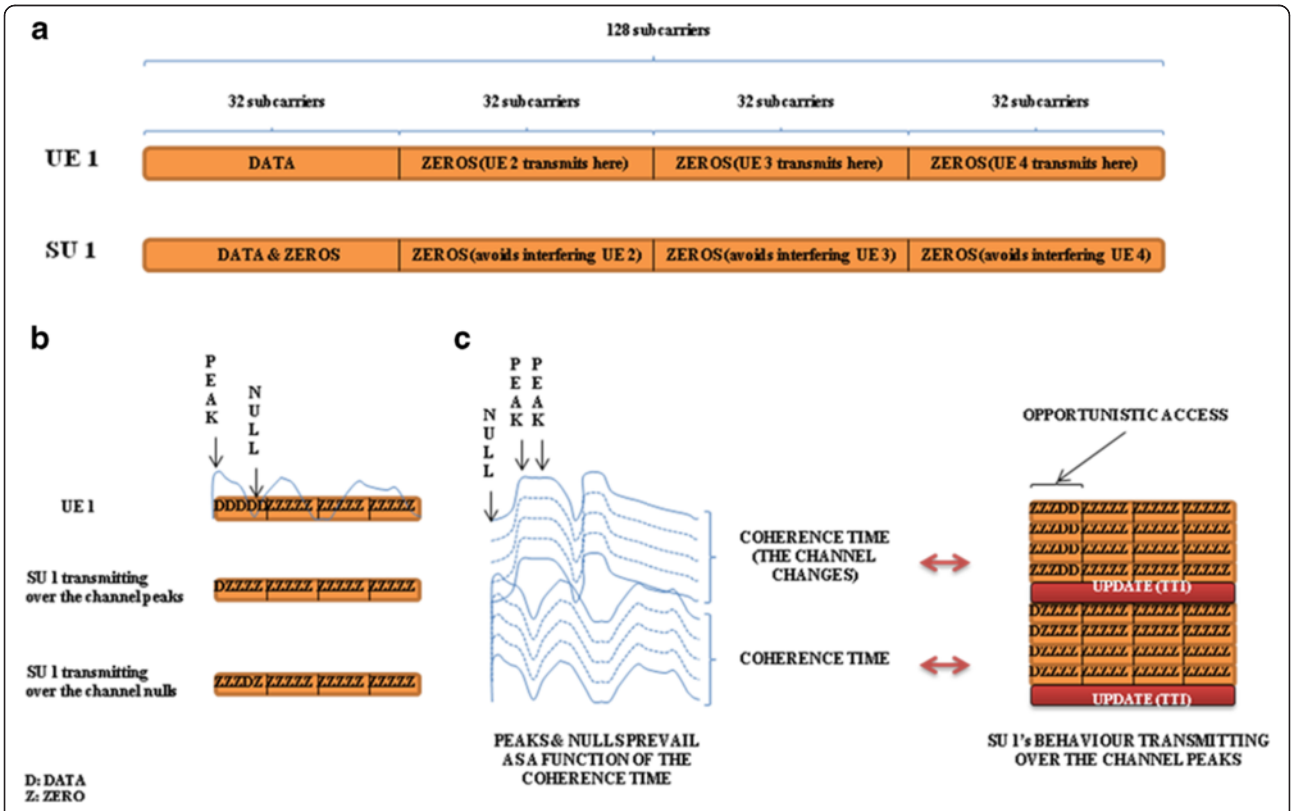

Figure 4 Schematic representation of an opportunistic secondary transmission carried out over the peaks/nulls of a mobile channel.

Table 2 Simulation parameters according to the 3GPP-LTE standard

Variable	Value	Description
p	128	Total number of subcarriers in the system
k	32	Number of subcarriers per user
q	4	Number of simultaneous transmissions (users) without co-channel interference
BW	1.4	Channel bandwidth (MHz)
T_s	0.52083	Sampling time (μs)
UE_speed	3-120	UE speed (km/h)
f_c	1850.7	Carrier frequency (MHz)

whom the channel changed about 48 times (coherence time approximately equal to 2.058 ms) within the same time interval.

On the other hand, it is important to mention that as part of the primary network there is an element playing an important role on the performance of the system, which is called channel scheduler [32-34]. In a broad sense, a channel scheduler is an algorithm that makes use of the channel state information provided by all the users in the system for taking decisions about which part (i.e., resource chunk) of the whole shared bandwidth is the most suitable one (in terms of channel conditions) for each user. A direct consequence of this has to do with a perceptible improvement at the moment of computing the system's error rate. So, with aiming at incorporating this element to the proposed scenario, the channel-dependent scheduler based on the algorithm so-called prioritized-bifacet Hungarian method (which offers an equivalent performance to the binary tree algorithm) has been utilized for this purpose [35].

The global view of the proposed scenario including the 3GPP-LTE primary network, and the presence of a SU awaiting for an opportunistic transmission are depicted in Figure 6.

In the network depicted above, the primary transmission corresponding to the UE1 (implemented according to the shown in Section 2.2.2) is assumed to have a direct relationship with the SU due to its mutual proximity. Thereafter, the implemented mobile channels can be observed, including the one corresponding to the SU moving at 3 km/h. Regarding the base station, in addition to its inherent functionalities, the presence of two elements can be highlighted: the channel scheduler and a CR receiver module. The channel scheduler deals with the optimal resolution about the use of the transmission bandwidth (information that is send as feedback to the active users including the SU), while the CR receiver module has to do with the cognitive radio capabilities added to the classic eNode-B for managing the opportunistic low-priority transmissions.

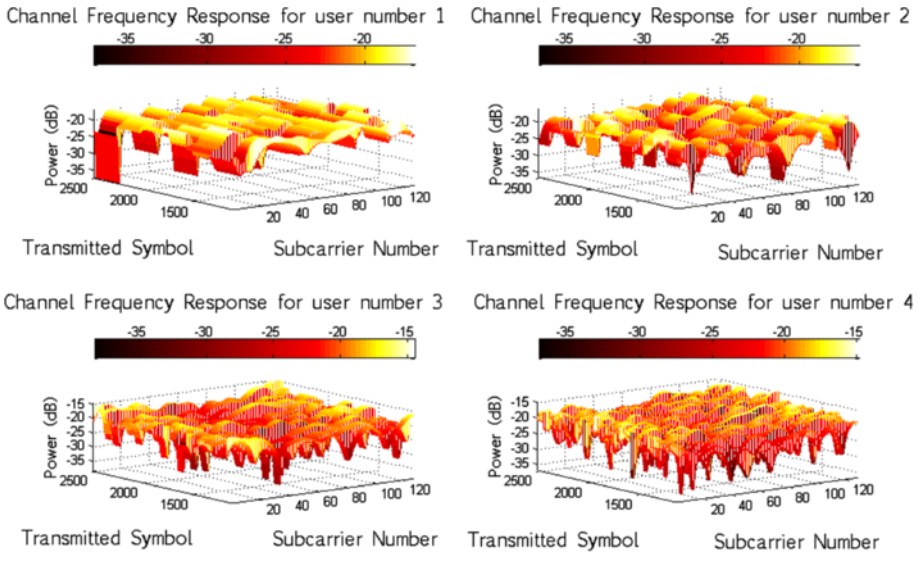

Figure 5 Figure 5 Frequency response, mobile channels corresponding to UE's operating at 1850.7 MHz moving at 15 Km/h, 30 Km/h, 60 Km/h, and 120 Km/h respectively.

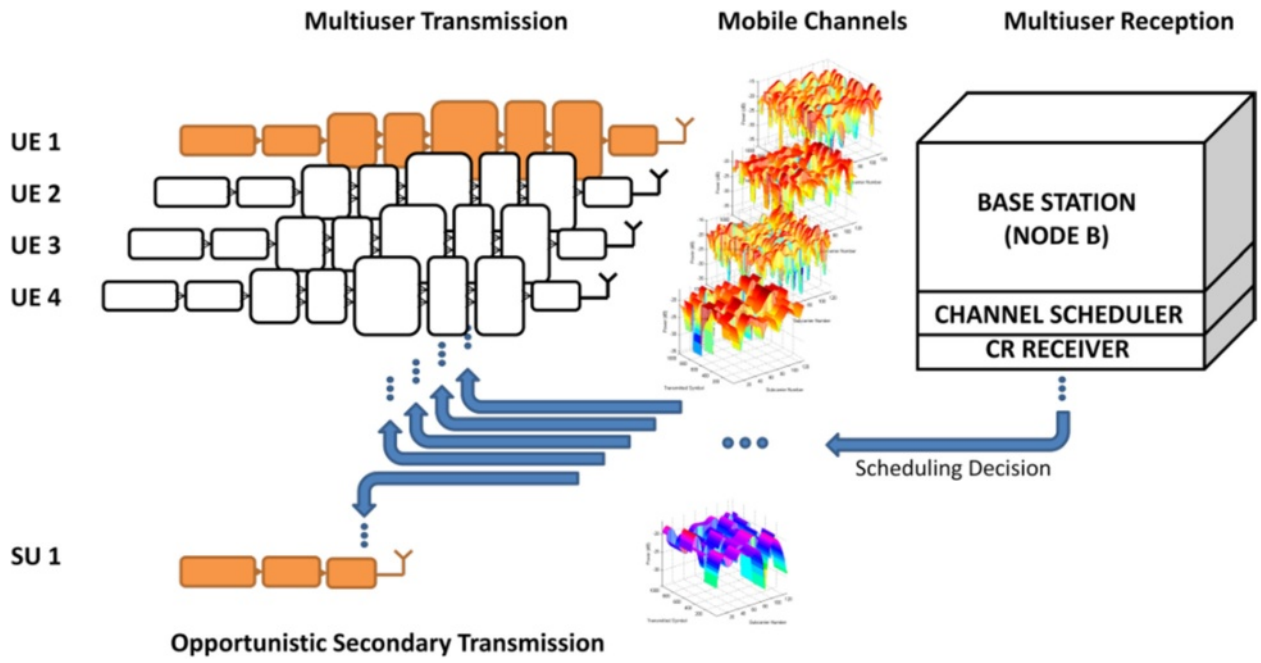

Figure 6 3GPP-LTE uplink scenario subject to the presence of a SU awaiting for transmission opportunity.

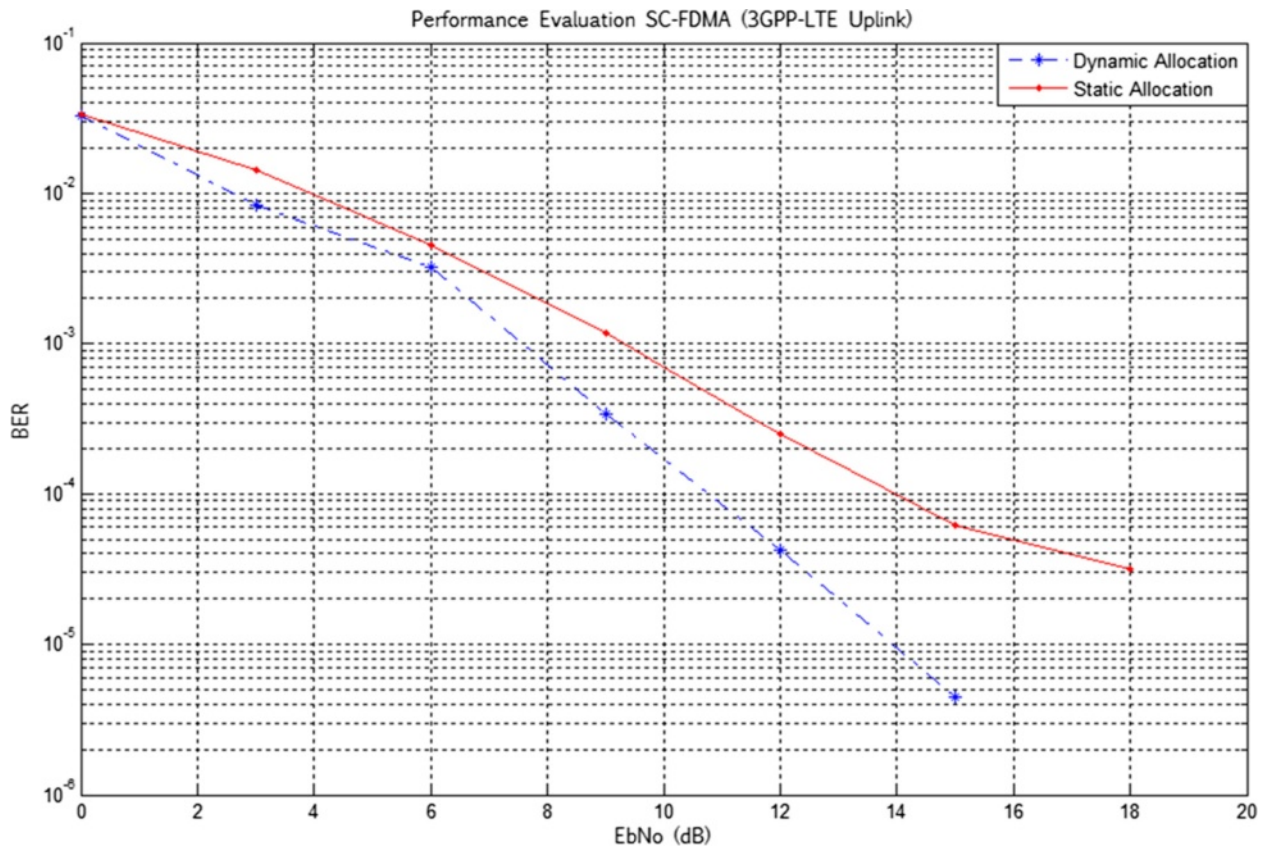

Figure 7 SC-FDMA system, performance evaluation of an uninterfered PU (fixed versus dynamic allocation of radio resources).

3. Obtained results

In this section, the performance of the PU being affected by the opportunistic overlaid communication by the cognitive radio user is evaluated. In addition to the specifications shown in Table 2, a normal cycle prefix, a localized mapping, and a modulation scheme given by Q-PSK were also considered [36]. Moreover, it is important to mention that for simulation purposes the 128 subcarriers were set available for transmission, being only 32 contiguous subcarriers allocated to each of the 4 active UEs (i.e., the channel scheduler manages resource chunks composed by 32 subcarriers). Highlighting that in real conditions not all the subcarriers are set available for transmission because some of them carry control signals, while some others (i.e., on edges) are unused in order to provide the required isolation to other bands [37]. Nevertheless, in our case no control signals are required because we assume perfect knowledge of the channel, while the perturbations caused to other systems in adjacent operation bands are neglected given that the idea of this proposal is not even to disturb in a significant manner the system under analysis.

The study presented here was made by considering static and dynamic allocations of radio resources. In this regard, and aiming at having a performance of reference, the BER of an uninterfered primary user was computed just as shown in Figure 7.

Every point on each of the curves above is the result of having transmitted 14,000 SC-FDMA symbols after having considered several E_bN_o (from 0 to 21 dB). The first thing to notice is the clear benefit of having added a dynamic allocation of resources to the LTE system (i.e., a channel-dependent scheduler), because the BER curve decreases faster with respect to the one built from a static allocation of bandwidth. That is, under a dynamic allocation of resources the system stops having errors with an E_bN_o greater than 15 dB, while in the other case this occurs after having an E_bN_o greater than 18 dB.

So, having these curves as reference, the channel information of a particular PU (i.e., UE in LTE) was tracked aiming at inducing an opportunistic communication taking place on its extreme conditions when $P = P_{SU}$. The interference was induced by two ways, the first one by overlaying secondary data exclusively on the subcarriers affected by a null, and the second one by doing exactly the opposite thing (i.e., by identifying the channel peaks).

Regarding the induced interference, two thresholds were selected aiming at enabling the secondary transmission (the thresholds were chosen as the maximums & minimums found in the channel by considering 14,000 transmissions). The total number of opportunities identified in each case is shown in Table 3.

Under the cognitive radio context, it is said that this type of technology is allowed to slightly disturb a primary communication [38,39]. In this regard, it can be observed that the fact of overlaying secondary data on the worst primary subcarriers (i.e., in terms of channel conditions) results in a very high interference for the UE, situation that is more and more evident as the E_bN_o increases. On the other hand, it can be noticed that carrying out a secondary transmission overlaid on the best subcarriers (i.e., channel peaks) does not distort the primary communication beyond the previously observed order of magnitude, and that when no errors are identified in the conventional transmission, the BER of the interfered one moves up to having approximately one error per every 1,000,000 of bits received (i.e., $\approx 1 \times 10^{-6}$).

A way of observing the opportunistic access of the cognitive radio transmitter is by plotting the SIR, which is shown in Figure 8 for the case of co-transmitting over the channel peaks when the E_bN_o is equal to 21 dB. Chosen because according to the analysis made before, the fact of transmitting over the best channel conditions seems to be the best strategy to be followed by a SU.

An inspection to the curve above will allow us to visualize the whole transmission in terms of time, frequency, and power. The fact that the output be concentrated on the left side of the x-axis has to do with the fixed allocation of radio resources (the eNodeB scheduled the first resource chunk to the UE in question all the time). On the other hand, by observing the y-axis

Table 3 UE's performance and the total number of discovered opportunities for the secondary user (static allocation)

E_bN_o (dB)	No interference BER	Nulls BER (total opportunities)	Peaks BER (total opportunities)
0	3.344×10^{-2}	4.38×10^{-2} (460)	3.903×10^{-2} (1610)
3	1.439×10^{-2}	1.263×10^{-2} (230)	1.148×10^{-2} (3910)
6	4.593×10^{-3}	5.879×10^{-3} (460)	4.019×10^{-3} (2760)
9	1.18×10^{-3}	2.01×10^{-3} (230)	1.487×10^{-3} (3450)
12	2.489×10^{-4}	8.147×10^{-5} (0)	2.254×10^{-4} (3450)
15	6.138×10^{-5}	2.892×10^{-3} (230)	3.192×10^{-5} (2070)
18	3.125×10^{-5}	5.46×10^{-3} (690)	4.129×10^{-5} (1610)
21	0	4.385×10^{-2} (460)	1.116×10^{-6} (2070)

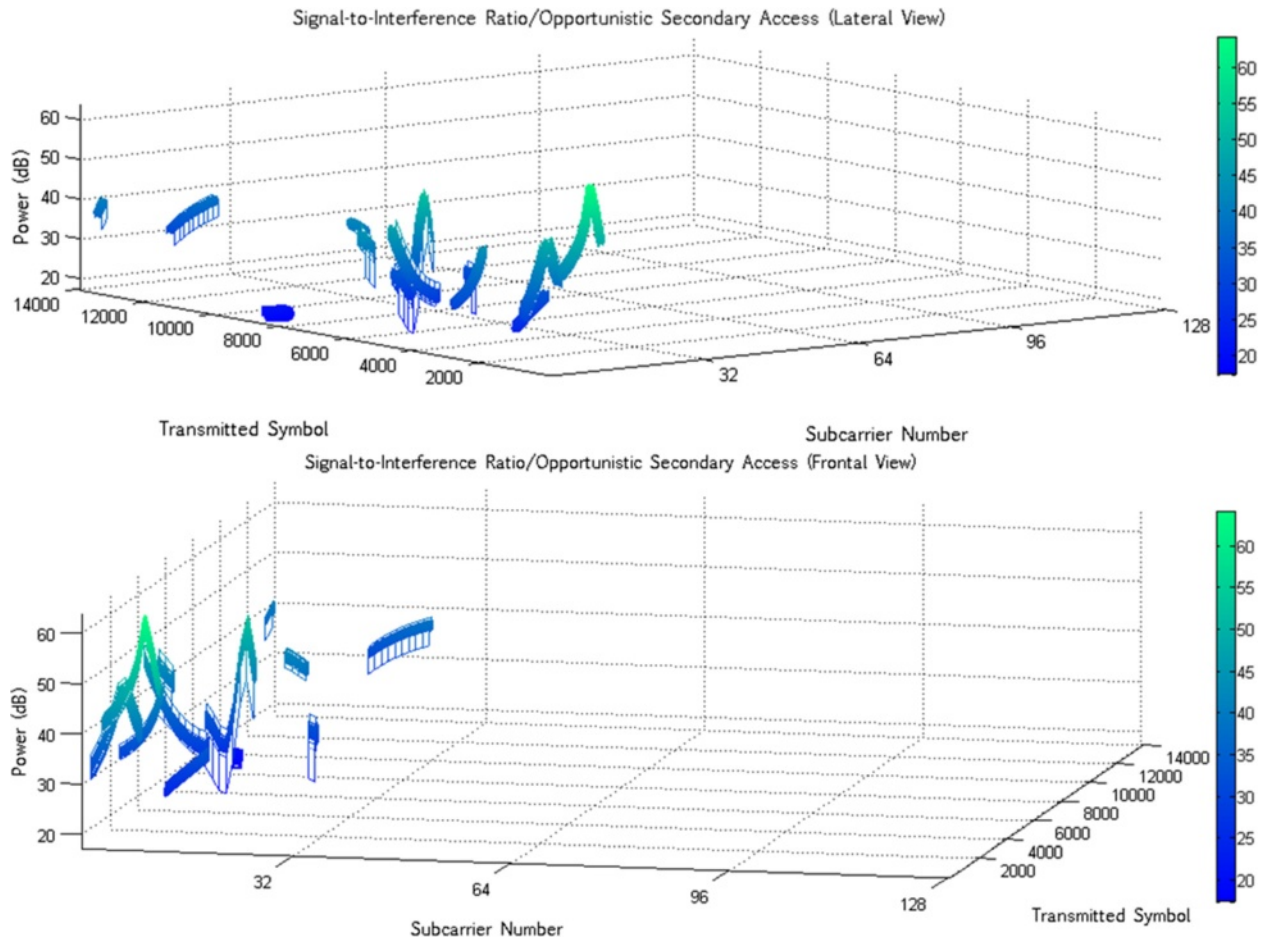

Figure 8 SIR of a UE subject to the interference produced by a SU co-transmitting over the peaks of a mobile channel (fixed allocation).

we can confirm the opportunistic access in terms of time (we know that in LTE the symbol length is 66.7 μs), while by giving a look at the *z*-axis we can see that the SIR kept high since the secondary communication was carried out through the channel peaks.

Once the proposal of co-transmitting over the extreme channel conditions was tested under a fixed allocation of radio resources, the same kind of analysis was carried out but this time by putting into operation a channel-dependent scheduler (i.e., a dynamic allocation of resources). Regarding the secondary transmissions, the thresholds were slightly moved (nulls from $|H_{\mathrm{PU}}|^2 <= 4 \times 10^{-8}$ to $|H_{\mathrm{PU}}|^2 <= 8 \times 10^{-8}$, peaks from $|H_{\mathrm{PU}}|^2 => 3 \times 10^{-4}$ to $|H_{\mathrm{PU}}|^2 => 5 \times 10^{-4}$), this because after the insertion of the channel scheduler the nulls are harder to be identified while the peaks are discovered in an easier way.

The total number of discovered opportunities when the dynamic allocation of radio resources is performed can be checked in Table 4.

The proposed model clearly states that only the subcarriers that are undergoing extreme channel conditions are those which will be used for secondary purposes (see Equation 6). Thus, the zeros on the table above make evident that sometimes no secondary access was granted, this because the extreme conditions taking place during such transmissions did not fulfill the stipulated by the thresholds that were previously shown.

As can be noticed from Table 4, the transmission over the channel nulls was performed twice. The third column on the table (nulls A) confirms that co-transmitting over the deep fadings increases the bit error rate of the primary system, while the fourth column (nulls B) illustrates that when no chances (or an insignificant number) were found, the BER follows the performance of the uninterfered communication. On the other hand, the last column shows that co-transmitting over the channel peaks leads to the discovery of more opportunities, while at the same time the performance of the primary user

Table 4 UE's performance and the total number of discovered opportunities for the secondary user (dynamic allocation)

E_bN_o (dB)	No interference BER	Nulls A BER (total opportunities)	Nulls B BER (total opportunities)	Peaks BER (total opportunities)
0	3.317×10^{-2}	3.192×10^{-2} (0)	2.584×10^{-2} (232)	3.367×10^{-2} (688)
3	8.415×10^{-3}	9.584×10^{-3} (230)	1.182×10^{-2} (460)	9.691×10^{-3} (230)
6	3.278×10^{-3}	2.938×10^{-3} (1)	8.387×10^{-3} (688)	3.794×10^{-3} (459)
9	3.404×10^{-4}	1.271×10^{-3} (231)	1.388×10^{-3} (235)	3.661×10^{-4} (1148)
12	4.241×10^{-5}	8.259×10^{-5} (1)	2.176×10^{-4} (232)	2.723×10^{-4} (687)
15	4.464×10^{-6}	3.467×10^{-3} (459)	3.348×10^{-6} (1)	4.576×10^{-5} (229)
18	0	0 (0)	0 (2)	0 (0)
21	0	2.112×10^{-3} (231)	0 (3)	1.004×10^{-5} (2294)

keeps less distorted (the errors do not grow up more than one order of magnitude, and when no opportunities are identified the bit error rate stays the same as the conventional one).

An interesting issue that was confirmed by this second experiment had to with the fact that even when the number of opportunities for co-transmitting over the nulls resulted to be much lesser than the number of chances for co-transmitting over the channel peaks, the distortion was considerably higher in the first case. An explanation to this behavior has to do with the equalizer embedded in the reception chain, which tends to amplify the induced interference that is located over the deep fadings.

So, aiming at testing this hypothesis, a mathematical analysis was performed for a MMSE subject to extreme channel conditions, which can be found in Appendix. The mathematical proof confirmed that an MMSE exposed to a channel null will provide a quite large weighting factor and hence will amplify the interference located on a deep

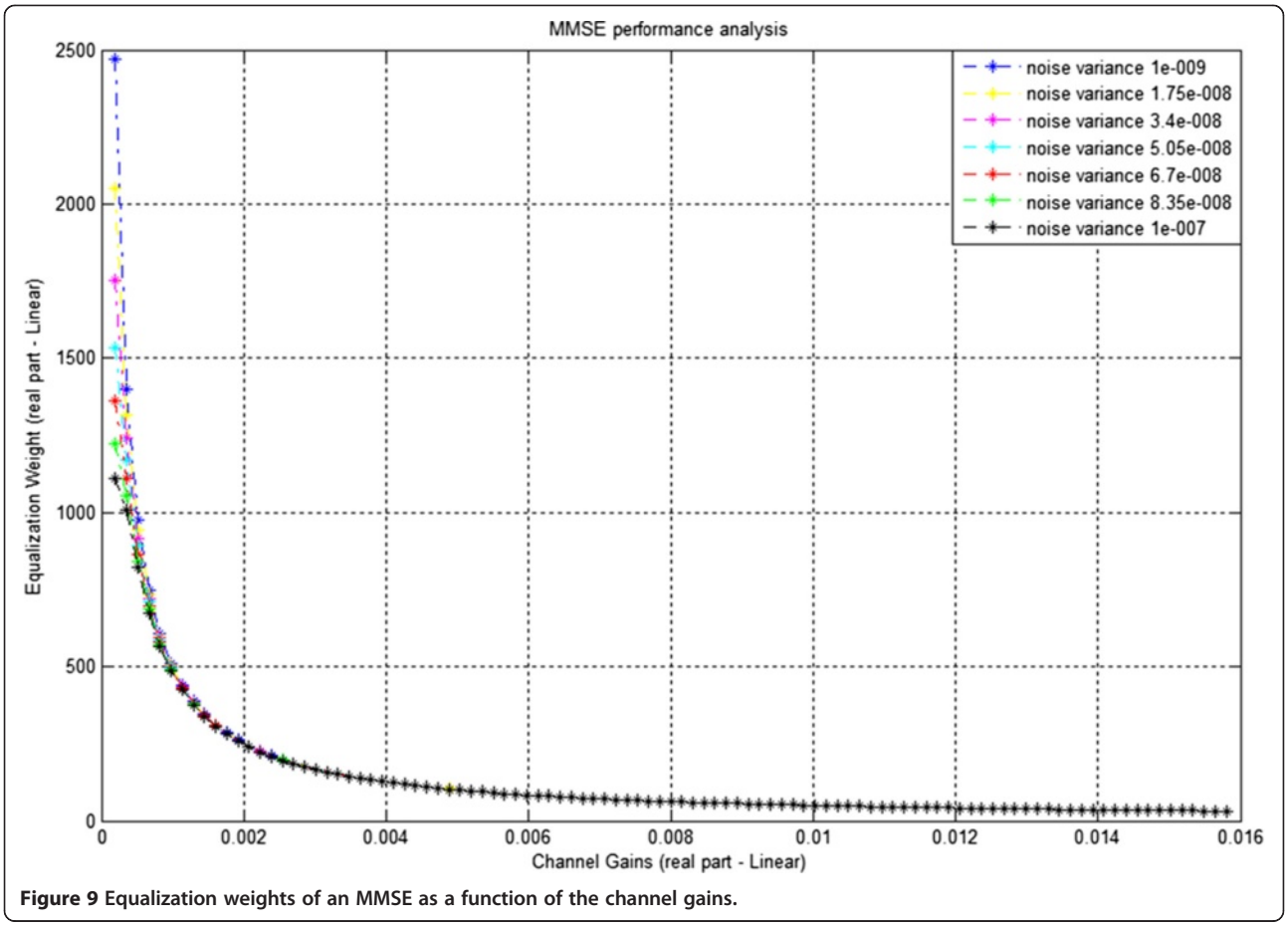

Figure 9 Equalization weights of an MMSE as a function of the channel gains.

fading. On the other hand, when the MMSE faces a channel peak the weighting factor will be very small, and therefore the induced interference will not be amplified. An analytical examination was also conducted just as can be seen in Figure 9.

The figure above shows a set of curves describing the output of an MMSE when different channel gains going from a null to a peak are considered (i.e., matching the range of the thresholds chosen in this study). In a broad sense, the obtained curves confirm what is mathematically demonstrated in Appendix, that an MMSE will provide a very high equalization weight when is exposed to a null, and that will do the opposite thing for a peak. Moreover, in the case of a null we can also note from the curves that as the E_bN_o be increased (i.e., the noise variance decreased), the MMSE will also provide each time a higher equalization weight and hence the induced interference will tend to cause more and more damage to the primary communication.

In Figure 10, the SIR was estimated for the case of co-transmitting over the channel peaks when dynamic allocation is put into operation.

About the figure above, since the eNodeB makes use of a channel-dependent scheduler, the first thing to notice is how the communication took place along the whole bandwidth (i.e., all the resource chunks were utilized by the UE under analysis). Consistently, we can see through the SIR curve that the secondary communication moved dynamically along the granted bandwidth always pursuing the UE in question (i.e., avoiding to interfere with the others).

4. Conclusions

An overlay cognitive radio communication which induces an opportunistic secondary communication through the small-scale fading mechanisms inherently present into the mobile channels was proposed here. The SC-FDMA system became in the study object of

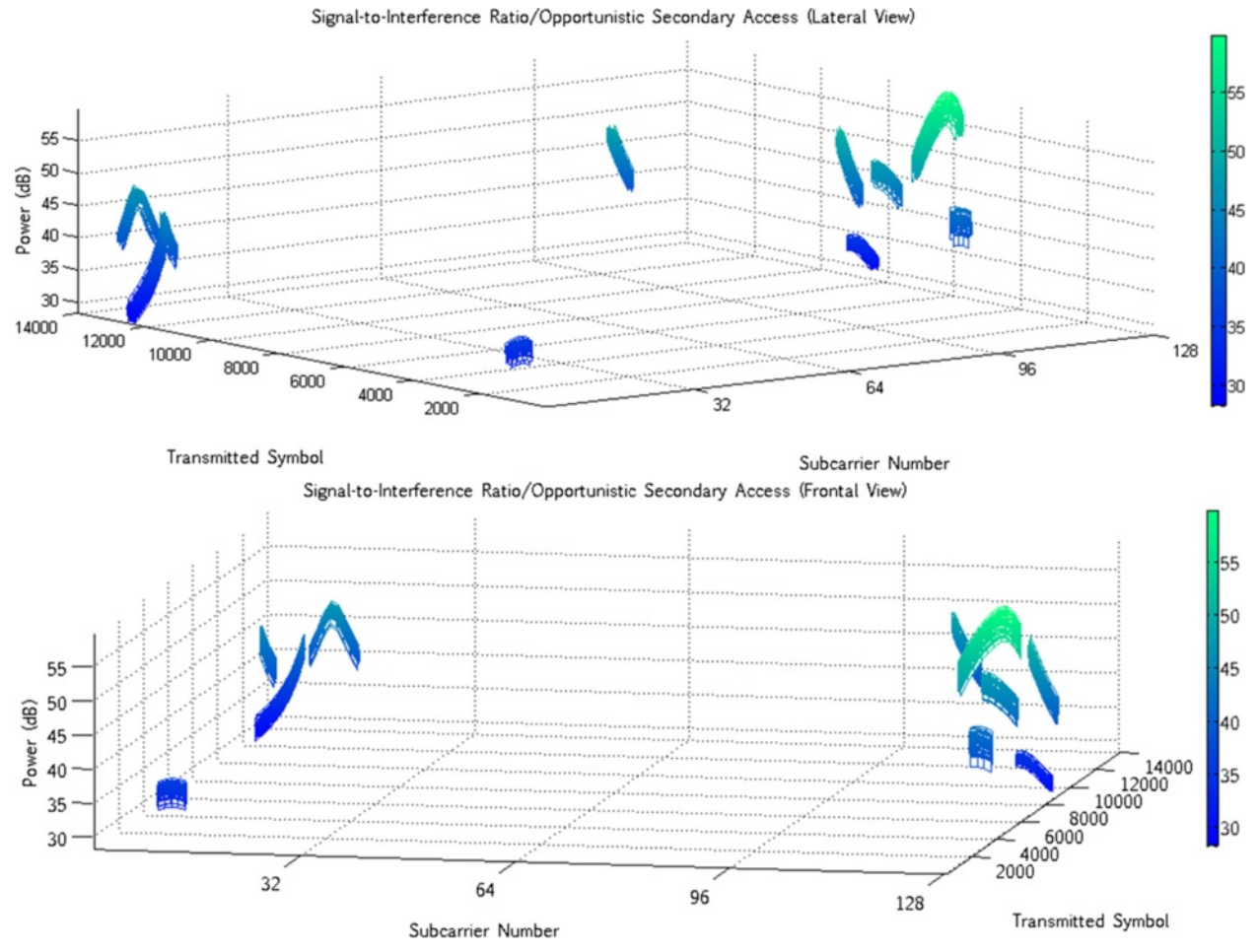

Figure 10 SIR of a UE subject to the interference produced by a SU co-transmitting over the peaks of a mobile channel (dynamic allocation).

this proposal, being the delay spread of the signal, and the time variance of the LTE mobile channel the crucial points of analysis. So, whereas the frequency selectivity of the channel provides the information about which subcarriers along the entire transmission bandwidth are undergoing the best, the worst, and intermediate conditions, the fading rapidity indicates (i.e., depending on the carrier frequency and UE speed) approximately how long time the conditions over those subcarriers will be steady. In this regard, the 3GPP-LTE technical specifications and the model given by Young and Beaulieu [20] were utilized for implementing an LTE mobile channel corresponding to an urban area. From the implemented channel it was possible to find that for a UE moving at 15 km/h and operating at 1850.7 MHz, the channel remains invariant approximately during 16.462 ms, which is equivalent to transmitting around 230 SC-FDMA symbols. Subsequently, and under these bases a multi-user mobile environment was implemented aiming at incorporating a CR user as a listener of the primary network, which was focused on opportunistically exploiting (and as function of the coherence time) the extreme conditions of the primary channel being tracked. So, the deployed scenario was analyzed by inducing opportunistic interference through the peaks and nulls of a primary channel, and under the static and dynamic allocations of radio frequency resources. From the system's performance evaluation, it was found that an overlay transmission through the channel nulls resulted in a much more significant degradation of the conventional transmission than the originated by opportunistically transmitting over the channel peaks, this is attributed to the MMSE equalizer embedded in the system. So, after finding that co-transmitting over the primary channel peaks seems to be a better choice for accessing to the primary resources, we can point out that in the case of the static allocation of resources the best interfered bit error rate we got was 1.116×10^{-6} with 21 dB, which is better than an un-interfered communication with 18 dB (3.125×10^{-5}). In the case of a dynamic allocation of resources the best interfered BER we got was 1.004×10^{-5}, which is certainly poorer than the one got previously, but we have to take into account that the threshold enabling the secondary access was modified (i.e., it was much more restrictive in the second case). We can conclude that of course there is a price to be paid at the moment of introducing a secondary communication in parallel; however, the operators could try to find a tradeoff aiming at receiving an extra benefit for having more costumers (i.e., secondary users paying fees) attached to their networks almost in a transparent way.

So, in order to conduct much more rigorous future studies about this proposal, the following issues have been selected as open challenges:

- To apply for example the extreme value theory on the provided channel gains aiming at determining the most suitable thresholds for enabling the CoRa communication.
- The implementation of a powerful error correction mechanism (e.g., a Turbo Code), aiming at evaluating the system performance under the proposed induced interference scheme.
- To carry out an analysis from the secondary user perspective (successive cancellation could be an attractive technique for recovering the overlapped data).
- To consider the analysis of real data (i.e., measured channels) aiming at identify the small-scale fading characteristics associated with this proposal.

In order to finalize, it has to be mentioned that constant speed cannot be assumed to happen in real-world situations, and that the number of discovered opportunities based on the coherence time estimation cannot be guaranteed as in theory. Nevertheless, at the end the feasibility of this proposal could follow the same operation principle as a channel-dependent scheduler, which takes its decisions about the channel conditions assuming that will prevail constant until the next transmission time interval.

Appendix

Analysis of an MMSE receiver subject to extreme channel conditions (proof)

According to the obtained results shown in Section 3, the fact of co-transmitting through the channel nulls of a primary LTE channel brings as a consequence a high distortion on the primary communication, while co-transmitting over the LTE channel peaks causes less distortions. So, in this section it is explained why this happens.

The σ^2 plays a fundamental role, which will be each time smaller as the performance of the communication be better and better (i.e., as the E_bN_o increases, the σ^2 will decrease until being almost equal to zero).

MMSE weighting factor and the channel nulls

Lets consider first that $\sigma^2 = 1 \times 10^{-3}$, hence the MMSE weighting factor would be.

$$G(k) = \frac{H(k)^*}{|H(k)|^2 + 1 \times 10^{-3}}, \tag{10}$$

Since a null is an extreme condition, lets consider a null as a channel gain that tends to zero.

$$\begin{aligned}\lim_{H(k)\to 0} G(k) &= \lim_{H(k)\to 0} \frac{H(k)^*}{|H(k)|^2 + 1\times 10^{-3}} \\ &= \lim_{H(k)\to 0} \frac{H(k)^*}{H(k)H(k)^* + 1\times 10^{-3}} \\ &= \lim_{H(k)\to 0} \frac{1}{H(k) + 1\times 10^{-3}}, \\ &= \lim_{H(k)\to 0} \frac{1}{1\times 10^{-3}} \\ &= 1000, \end{aligned} \tag{11}$$

And when $\sigma^2 = 1\times 10^{-9}$,

$$\begin{aligned}\lim_{H(k)\to 0} G(k) &= \lim_{H(k)\to 0} \frac{H(k)^*}{|H(k)|^2 + 1\times 10^{-9}} \\ &= \lim_{H(k)\to 0} \frac{H(k)^*}{H(k)H(k)^* + 1\times 10^{-9}} \\ &= \lim_{H(k)\to 0} \frac{1}{H(k) + 1\times 10^{-9}}, \\ &= \lim_{H(k)\to 0} \frac{1}{1\times 10^{-9}} \\ &= 1000000000 \end{aligned} \tag{12}$$

The above analysis tells us that when the equalizer is dealing with channel nulls it will try to compensate such deep fadings by providing a large weighting factor, which will depend on the σ^2 in question.

MMSE weighting factor and the channel peaks

Another extreme condition lays in the fact of co-transmitting through the channel peaks. Here for demonstration purposes we will consider a peak as a channel gain tending to infinite, and because of that, it does not matter how small is the value of σ^2. So, under these assumptions lets see what happen with the weighting factor of the MMSE.

$$\begin{aligned}\lim_{H(k)\to \infty} G(k) &= \lim_{H(k)\to \infty} \frac{H(k)^*}{|H(k)|^2 + \sigma^2} \\ &= \lim_{H(k)\to \infty} \frac{H(k)^*}{H(k)H(k)^* + \sigma^2} \\ &= \lim_{H(k)\to \infty} \frac{1}{H(k) + \sigma^2}, \\ &= \lim_{H(k)\to \infty} \frac{1}{\infty} \\ &= 0 \end{aligned} \tag{13}$$

As we can see in equation 13, when the channel gain approaches infinity (i.e., representing a peak on the channel), the weighting factor approaches zero. That is, in such cases the MMSE has nothing to compensate because the channel conditions are pretty good.

Conclusions about the MMSE weighting factor and the extreme conditions (nulls & peaks) in a channel

We can conclude that when we place secondary data over the nulls of a primary channel, the MMSE at the receiver will increase the interference and hence the performance of the primary communication will be degraded, situation that tends to be more and more severe as the E_bN_o increases.

On the other hand, if a secondary user co-transmits exclusively over the channel peaks, the induced interference will not significantly be increased. This MMSE would be dealing with a quite large channel gain, and hence the weighting factor would be very small (in fact we saw that no compensation is provided by the MMSE when the channel gain is hypothetically taken as infinite).

So, if a secondary user is going to transmit opportunistically through the extreme conditions of a primary channel, a better strategy would be co-transmitting over the channel peaks.

Competing interests

The authors declare that they have no competing interests.

Acknowledgments

The authors would like to thank the Technical University of Catalonia (UPC), the Aalto University School of Science and Technology, the COST Action IC0905 TERRA (because part of this work was presented there), and the National Council of Science and Technology in Mexico (CONACYT) for the financial support granted.

Author details

[1]Barcelona-Tech, Signal Theory and Communications Department, Technical University of Catalonia, Building D4, Campus Nord, Jordi Girona 31, 08034, Barcelona, Spain. [2]Department of Radio Science and Engineering, Aalto University School of Science and Technology, Otakaari 5A, Espoo 02015, Finland.

Received: 21 May 2012 Accepted: 18 February 2013
Published: 25 March 2013

References

1. TS Rappaport, *Wireless Communications* (Prentice Hall, NJ, 1996), pp. 69–196
2. Y Okumura, E Ohmori, T Kawano, K Fukuda, Field strength and its variability in UHF and VHF land-mobile radio service. Rev. Electric. Commun. Lab. **16**(9), 825–873 (1968)
3. European Co-operative in the Field of Science and Technical Research, Urban transmission loss models for mobile radio in the 900 and 1800 MHz bands, Technical Report, EURO COST 231. September 1991
4. HL Bertoni, W Honcharenko, LR Macel, HH Xia, UHF propagation prediction for wireless personal communications. Proc. IEEE **82**, 1333–1359 (1994)
5. S Haykin, M Moher, *Modern Wireless Communications* (Prentice Hall, NJ, 2005)
6. D Tse, P Viswanath, *Fundamentals of Wireless Communications* (Cambridge University Press, Cambridge, MA, 2005)
7. A Goldsmith, *Wireless Communications* (Cambridge University Press, Cambridge, MA, 2005), pp. 190–209
8. HL Bertoni, *Radio Propagation for Modern Wireless Systems (Prentice* (NJ, Hall, 2000)
9. F Belloni, *Postgraduate course in radio communications, Fading Models* (Helsinki University of Technology, 2004). http://www.comlab.hut.fi/opetus/333/2004_2005_slides/Fading_models_text.pdf, Accessed September 2011
10. WC Jakes, *Microwave Mobile Communications* (IEEE Press, New York, 1974)

11. A Papoulis, *Probability Random Variables, and Stochastic Processes*, 3rd edn. (McGraw-Hill, New York, 1991)
12. JG Proakis, *Digital Communications*, 2nd edn. (McGraw-Hill, New York, 1989)
13. M Ptzold, *Mobile Fading Channels* (Wiley, New York, 2002)
14. B Sklar, Rayleigh fading channels in mobile digital communications systems. Part 1: characterization. IEEE Commun. Mag. **35**(7), 90–100 (1997)
15. JD Parsons, *The Mobile Radio Propagation Channel*, 2nd edn. (Wiley, New York, 2000)
16. PM Shankar, *Introduction to Wireless Systems* (Wiley, New York, 2002)
17. PA Bello, Characterization of randomly time-variant linear channels. IEEE Trans. Commun. Syst. **CS-11**, 360–393 (1963)
18. 3GPP TS 45.005 V9.3.0, *Radio Access Network: Radio Transmission and Reception*, 2010
19. HG Myung, DJ Goodman, *Single Carrier FDMA: A New Air Interface for Long Term Evolution* (Wiley, New York, 2008)
20. DJ Young, NC Beaulieu, The generation of correlated Rayleigh random variates by inverse discrete Fourier transform. IEEE Trans. Commun **48**, 1114–1127 (2000)
21. JI Smith, A computer generated multipath fading simulations for mobile radio. IEEE Trans. Veh. Technol. **VT-24**, 39–40 (1975)
22. D Greenwood, L Hanzo, *Characterisation of Mobile Radio Channels, Mobile Radio Communications* (Pentech Press, London, 1994)
23. 3GPP TS 36.211 V9.1.0, *Physical Channels and Modulation*, 2010
24. HG Myung, J Lim, DJ Goodman, Single carrier FDMA for uplink wireless transmission. IEEE Veh. Technol. Mag **1**(3), 30–38 (2006)
25. BE Priyanto, H Codina, S Rene, TB Sorensen, P Mogensen, Initial performance evaluation of DFT-spread OFDM based SC-FDMA for UTRA LTE uplink, in *Proceedings of IEEE 65th Vehicular Technology Conference, VTC 2007-Spring*, 2007, pp. 3175–3179. 22–25 April 2007
26. M Ergen, *Mobile Broadband, Including WiMAX and LTE* (Springer, New York, 2009), pp. 261–266
27. HG Myung, Introduction to single carrier FDMA, in *15th European Signal Processing Conference (EUSIPCO) 2007* (Poznan, Poland, 2007)
28. H Ekström, A Furuskär, J Karlsson, M Meyer, S Parkvall, J Torsner, M Wahlqvist, Technical solutions for the 3G long-term evolution. IEEE Commun. Mag. **44**(3), 38–45 (2006)
29. F Khan, *LTE for 4G Mobile Broadband, Air Interface Technologies and Performance* (Cambridge Press, Cambridge, UK, 2009), pp. 70–87
30. 3GPP TR 25.814 V7.1.0, *Physical Layer aspects for evolved Universal Terrestrial Radio Access (UTRA)*, 2006
31. 3GPP TR 25.943 V9.0.0, *Technical Specification Group Radio Access Network: Deployment aspects*, 2009
32. J Lim, HG Myung, K Oh, DJ Goodman, Channel-dependent scheduling of uplink single carrier FDMA systems, in *IEEE Proceedings of the Vehicular Technology Conference, VTC-2006 Fall*, 2006, pp. 1–5. 25–28 September
33. L Ruiz de Termino, Channel-aware scheduling algorithms for SC-FDMA in LTE uplink, in *IEEE 19th International Symposium on PIMRC 2008*, 2008, pp. 1–6. 15–18 September
34. K Tahboub, *Comparison of channel dependent scheduling policies in LTE uplink* (Purdue University, West Lafayette, Indiana, 2010). http://wenku.baidu.com/view/3a8ac3c1bb4cf7ec4afed0ba.html. Accessed 10 April 2010
35. GA Medina-Acosta, JA Delgado-Penín, On the feasibility of a channel-dependent scheduling for the SC-FDMA in 3GPP-LTE (mobile environment) based on a prioritized-bifacet hungarian method. EURASIP J. Wirel. Commun. Netw. **2011**, 71 (2011)
36. K Sung-won, K Kun-yong, Physical layer verification for 3GPP LTE (FDD), in *11th International Conference on Advanced Communication Technology.* ICACT **02**, 1095–1100 (2009). 15–18 February 2009
37. H Holma, A Toskala, *LTE for UMTS OFDMA and SC-FDMA Based Radio Access* (Wiley, Chichester, UK, 2009), pp. 76–80
38. AF Molisch, LJ Greenstein, M Shafi, Propagation issues for cognitive radio. Proc. IEEE **97**, 787–804 (2009)
39. Z Tabakovic, S Grgic, M Grgic, Dynamic spectrum access in cognitive radio, in *Proceedings of the 51st International Symposium ELMAR-2009* (Croatia, Zadar). 28–30 September 2009

doi:10.1186/1687-1499-2013-87
Cite this article as: Medina-Acosta *et al.*: An opportunistic cognitive radio communication through the exploitation of the small-scale fading mechanisms of the LTE mobile channel. *EURASIP Journal on Wireless Communications and Networking* 2013 **2013**:87.